EXPERIMENTAL AERODYNAMIC CHARACTERISTICS OF THE AIRFOILS LA 5055 AND DU 86-084/18 AT LOW REYNOLDS NUMBERS

by

L.M.M. Boermans
F.J. Donker Duyvis
J.L. van Ingen
W.A. Timmer

Experimental aerodynamic characteristics of the airfoils LA 5055 and DU 86-084/18 at low Reynolds numbers

L.M.M. Boermans
F.J. Donker Duyvis
J.L. van Ingen
Faculty of Aerospace Engineering
Delft University of Technology

W.A. Timmer
Institute for Windenergy
Delft University of Technology

Abstract

In the Low-Speed Low-Turbulence Wind Tunnel (LTT) of the Low Speed Laboratory (LSL) at Delft University of Technology experimental results have been obtained for two low Reynolds number airfoils with different means of laminar separation- and transition control: airfoil LA 5055 designed by Liebeck and airfoil DU 86-084/18 designed at LSL.

Lift and pitching-moment data were obtained from pressure measurements (LA 5055) and balance measurements (DU 86-084/18) and drag data from wake surveys. The fluorescent oil flow technique was used to visualize the flow behaviour.

Design features of the LA 5055 airfoil are a distinct destabilizing region between 27% and 47% chord followed by a Stratford type pressure recovery distribution. To prevent early separation near the tunnel walls, suction was applied in a small region on the walls along the airfoil contour. In spite of the destabilizing region, drag producing laminar separation bubbles were present, and drag reductions up to 33% were measured by applying a zig-zag tape turbulator for transition control. The maximum lift coefficient, being governed by the Stratford limiting pressure distribution, could be raised by 38% with semi triangular vortex generators positioned at 20% chord.

The DU 86-084/18 airfoil with 18% chord camber changing flap has been designed for application in radio-controlled model sailplanes of the F3B (multi-task) class. Similar to the design of modern sailplane wing airfoils, artificial transition control as well as flap deflections were integrated from the start into the design. Due to the presence of long laminar flow regions on the upper and lower surface, the effectiveness of zig-zag tape turbulators, and the camber changing flap, low drag values were obtained at the C_L- and Re-range of interest for this class of model airplanes. In addition, stalling behaviour was gradual at all flap deflections.
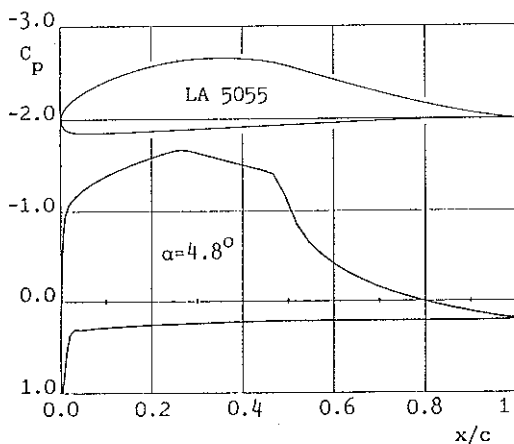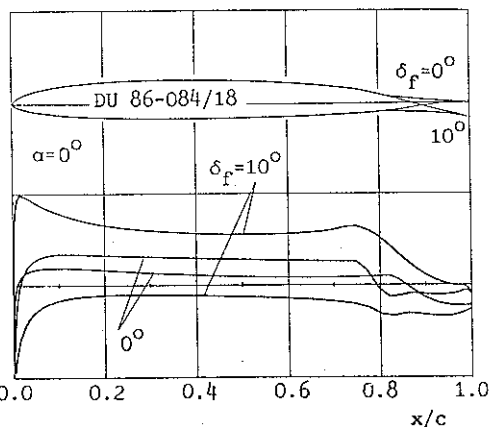
1. Airfoils

Fig. 1 Airfoil LA 5055

Fig. 2 Airfoil DU 86-084/18

The LA 5055 airfoil, designed by R.H. Liebeck, is characterized by an upper surface pressure distribution consisting of a rooftop with destabilizing region and a Stratford type pressure recovery distribution, Fig. 1. The destabalizing region is relatively long, from 27% chord to 47% chord, in the interest of promoting natural transition. The pressure recovery distribution was designed to take advantage of the conservatism in the Stratford distribution at low Reynolds numbers, as noted by Liebeck from windtunnel tests. The design conditions for LA 5055 were C_ℓ = 1.04 at α = 4.82⁰ and Re_c=0.6*10^6. The airfoil thickness is 15% chord.
The airfoil DU 86-084/18, Fig. 2, has been designed at LSL for application in radio controlled model sailplanes of the FAI F3B Class.

Competition in this class is focussed on speed (i.e. the time needed to fly four laps of 150 m and three turns), distance (i.e. the number of 150 m laps flown in four minutes) and duration (staying up and landing between marks after 6 minutes). A special winch launch technique is used to maximize altitude: after the initial climb phase a dive toward the winch is performed where maximum winch power and elasticity of the nylon line are converted to speed, and after disconnection a steep pull-up manoeuvre is used to convert this kinetic energy to potential energy for maximum altitude. The wings are built of carbon fiber material to withstand the high g-loadings during the pull-up manoeuvre.

Performance analysis shows that the range of operation for the airfoil is between lift coefficients of about 1 and 0 at corresponding Reynolds numbers of about 10^5 to 10^6. Low drag is emphasized in particular at lift coefficients below 0.5 (start, speed task and distance task), and a gradual stalling behaviour is required in view of the handling qualities in thermal flight conditions (duration task).

The LSL airfoil analysis and design computer program, Ref. 1,2,3, was used to design the airfoil. As shown in Fig. 2, the airfoil is relatively thin (8.4%c), has very long laminar flow regions on upper and lower surface, and a camber changing flap of 18%c. Similar to the design of modern sailplane wing airfoils, flap deflections and artificial transition control are integrated from the start into the design.

As indicated in the figure, the lower surface has been designed at the zero degree high speed flap deflection for laminar flow up to the flap, and the upper surface has been designed at the ten degree low speed flap deflection aiming at a long laminar flow region and a limited growth of the turbulent separated area at lift coefficients above the low drag bucket. The idea of the latter constraint is to avoid a dip in the lift versus angle of attack curve and accompanying bad handling and climbing qualities in thermal flight conditions; however, this sets a limit to the pressure gradient on the rear of the airfoil and thus the length of the laminar flow region.

As clarified in Ref. 4, artificial transition control to eliminate detrimental laminar separation bubbles, is preferable to the destabilizing region concept if an airfoil is required with a wide operating range of Reynolds numbers, lift coefficients and flap deflections, as in the present case. On the upper surface fixation of the laminar separation point, needed for the application of turbulators, is easily obtained by the change in pressure gradient at 75%c. On the lower surface this is the case at 82%c for the zero degree flap deflection only; the pressures induced by downward flap deflections will cause the laminar separation point to move forward,

thus making mechanical turbulators ineffective when they are submerged into the separated flow of the bubble. However, extensive tests with mechanical and pneumatic turbulators on a sailplane airfoil with similar lower surface pressure distribution (Ref. 3) did not reveal a drag increase due to this type of turbulator malfunction. Probably the additional pressures due to the bubble, acting over the corner in the contour at the flap hinge have no component in flow direction and hence no additional pressure drag exists.

Both the LA 5055 and the DU 86-084/18 airfoil were tested with zig-zag tape turbulators, which are the thinnest effective mechanical turbulators known to the authors, Ref 3.

2. Experimental Arrangement

Models

The LA 5055 airfoil model was cast in 3 equal, spanwise parts using a movable, accurate mould; casting material was the synthetic resin Araldit. The model has a chord length of 360 mm and is positioned vertically, spanning the 1.25 m height of the windtunnel test section. A total of 106 pressure orifices with diameter 0.4 mm and drilled perpendicular to the surface was located in staggered formation at the midspan station. In addition, 25 pressure orifices were located at 40 mm from each model end, to detect any wall-induced separation. Accuracy of the model contour was not measured, however, previous models made by this casting technique showed tolerances generally within 0.1 mm.

The DU 86-084/18 airfoil model consisted of an aluminum core surrounded by epoxy resin and thin layers of carbon and glass fiber fabric with a gel topcoat forming the aerodynamic surface. It was built in female mould halves for the upper and lower surface, which in turn were carefully produced with the help of machined templates. After the model was built in one piece, the flap was cut out and provided with a tubular nose and five center-hinges. The model has a chord length of 235 mm and is positioned vertically between reflection plates which are 0.60 m apart. Contour accuracy has not been measured yet, but inspection with the help of machined templates indicate that tolerance is tight.

Wind Tunnel and Instrumentation

The Low-Speed Low-Turbulence Wind Tunnel is of the closed return type with a contraction ratio of 17.9. The free-stream turbulence level in the test section varies from about 0.015% at 10 m/s to 0.045% at 60 m/s. The interchangeable octagonal test section is 1.80 m wide, 1.25 m high and 2.70 m long.

The LA 5055 model was attached to mechanically actuated turntables which are flush with the test section top and bottom wall, Fig. 3. Suction boxes with perforated plates were integrated into the turntables, providing attachment for the model as well.

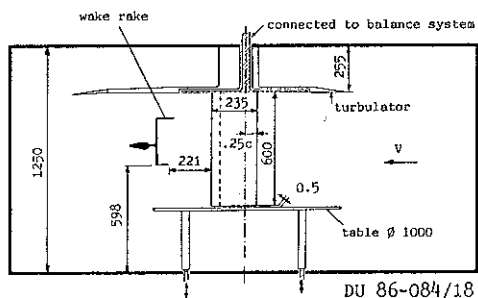

Fig. 3 LA 5055 test set-up   Fig. 4 DU 86-084/18 test set-up

The DU 86-084/18 model was attached vertically with one tip to a turntable, which is flush with a large reflection plate near the top wall; model and turntable are suspended to the windtunnel six component balance system, Fig. 4. A lower reflexion plate was present which left a small gap (0.5 mm) between the plate and the model tip.

In both cases, a wake rake, mounted on a cross beam and utilizing 50 total pressure tubes and 12 static pressure tubes, was used. Wakes were measured at 60%c and 95%c behind the trailing edge of LA 5055 and DU 86-084/18 respectively. All pressures were recorded by an automatically reading multi-tube liquid manometer (200 tubes). Pressure and balance data were on-line reduced using the Hp-21 MX-E laboratory computer.

Tests and methods

The LA 5055 model was tested in smooth condition at Reynolds numbers based on airfoil chord of $0.5*10^6$, $1*10^6$ and $1.5*10^6$. Strips of turbulator tape were used at Reynolds numbers of $0.5*10^6$ and $1*10^6$. The tape was 0.25 mm thick and 11 mm in width, and either unchanged, or cut in zig-zag form, Fig. 5.

To prevent early separation near the tunnel walls, suction of the tunnel wall boundary layer in the vicinity of the model was tested.

For that purpose the perforated plates were covered with adhesive plastic film except for the areas where suction was wanted.
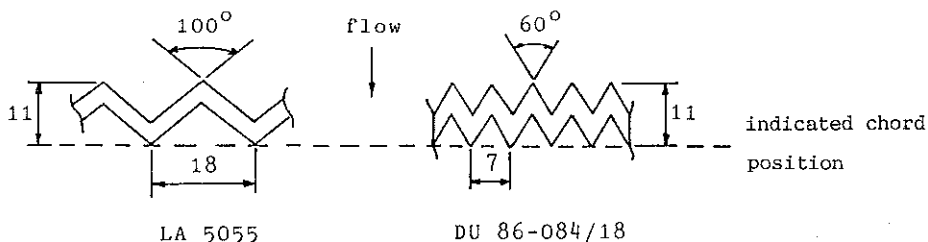

Fig. 5 Zig-zag tape turbulators

Finally, tests were performed with semi-triangular counter-rotating vortex generators positioned at 20%c, 30%c and 40%c. The vortex generators were similar to the devices used in Ref. 5, but the size was adapted for present purpose according to the recommendations of Ref 6. As shown in Fig. 6, the vortex generators were easily made by cutting and folding a thin brass strip.
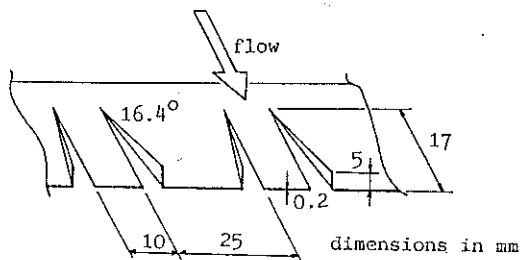

Fig. 6 Semi-triangular vortex generators

The Du 86-084/18 model was tested at Reynolds numbers from $0.2*10^6$ to $1*10^6$ and flap deflections from -5° to $+15^o$ both in smooth condition and with zig-zag tape turbulators, Fig. 5, on the upper and lower surface. On the upper surface 0.5 mm thick zig-zag turbulators were tested at positions between 67%c and 75%c, and on the lower surface 0.4 mm and 0.5 mm thick turbulators were tested at positions between 75%c and 79%c. The slots of the flap were sealed with tape of 0.04 mm thickness.

Laminar separation bubbles, turbulent separation and the effect of turbulators were visualized using the fluorescent oil-flow technique.

The static pressure measurements on the LA 5055 model surface were reduced to standard pressure coefficients and numerically integrated to obtain section normal force and pitching moment coefficients. For

the DU 86-084/18 model section normal force coefficients were obtained from the balance measurements taking the drag component of the turn-table (without model) into account. In both cases, profile drag coefficients were computed from the wake rake total and static pres-sures by the method of Jones, ref. 7.

In case of the LA 5055 measurements, standard low speed wind tunnel boundary corrections (Ref. 8) composed of solid and wake blockage, lift interference and wake-buoyancy, were applied to the section characteristics and pressure distributions. As an indication; the correction on the coefficients amount to less than 2% and on the angle of attack less than 0.2°. In case of the DU 86-084/18 measurements, no corrections were applied to the data because their magnitude is negligible. In both cases, the uncorrected coefficients are referred to the apparent dynamic pressure as measured without model at the center of the test section (standard procedure).

3. Experimental Results

LA 5055

The pressure distributions near the tunnel walls without suction showed early wall induced separation; this separation expanded to the midspan section and degraded the airfoil's performance at higher angle of attack, as shown in Fig. 7. Attempting to obtain instantaneous flow separation on the complete model, suction was applied in various
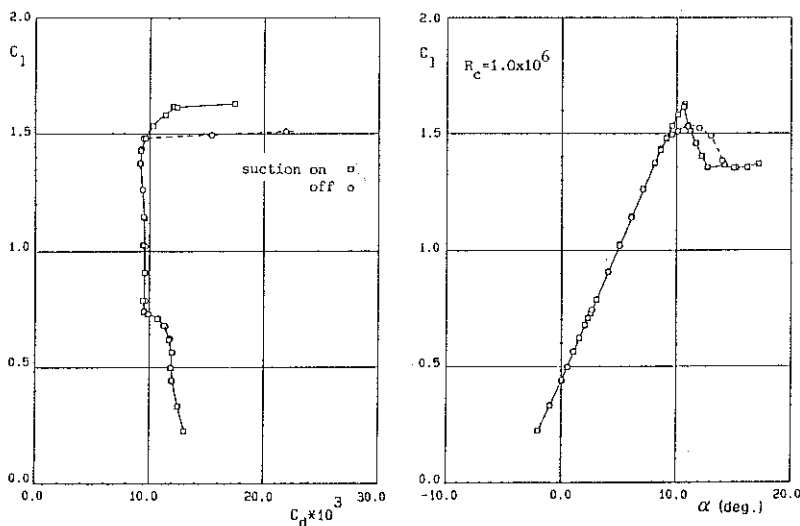
Fig. 7   Measured characteristics of LA 5055 with and without wall boundary layer suction

regions on the walls in front of the model as well as along the airfoil contour. The highest $C_{\ell_{max}}$ at the midspan section was obtained at every Re-number by suction in a 5 mm wide region along the airfoil upper surface, however, a perfect 2-D stall could not be obtain since separation started near the upper wall and rapidly progressed toward the lower wall. Stall near the upper wall could be postponed with a pair of counter-rotating vortex generators at 30%c, however no differences at the midspan section were detected.

At five different angles of attack (Re=0.5*10^6) spanwise drag surveys were made to check the two-dimensionality of the flow and to find a wake rake position where the drag represents a mean value. Some
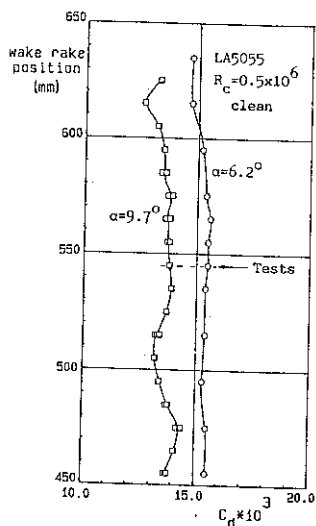

Fig. 8   Spanwise drag traverse
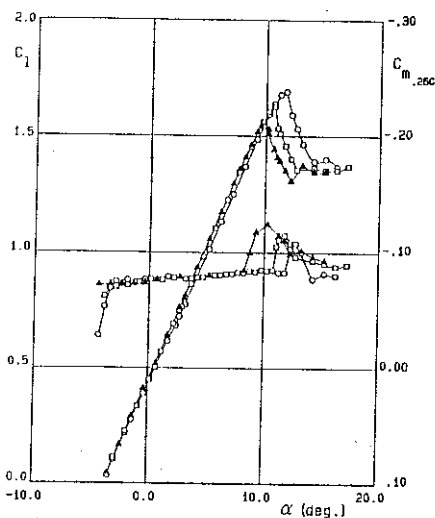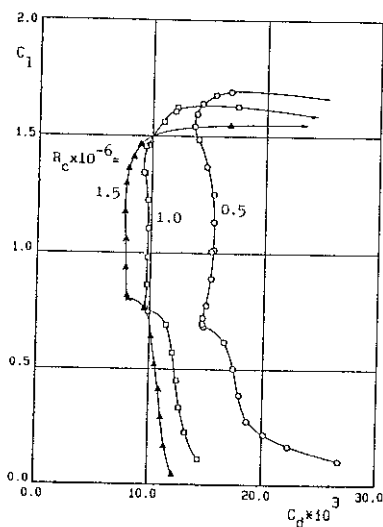   measurements, LA 5055
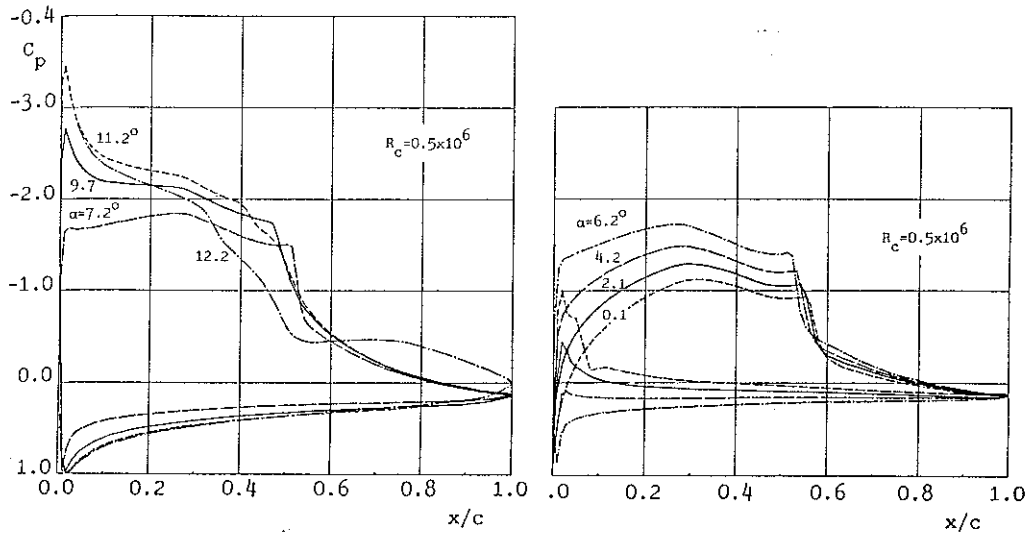

Fig. 9   Measured characteristics of LA 5055

Fig. 10 Measured pressure distributions of LA 5055.

typical results are shown in Fig. 8; spanwise variations in drag coefficient are generally less than 0.002. The wake rake was set at the position indicated in the figure.

Fig. 9 shows the measured aerodynamic characteristics at $Re=0.5*10^6$, $1*10^6$ and $1.5*10^6$. The flow behaviour at $Re=0.5*10^6$ is illustrated by the pressure distributions in Fig. 10. The flow on the lower surface is laminar up to the trailing edge at angles of attack higher than 2^0 i.e. the lower end of the low drag bucket, while at lower angles of attack there is a laminar separation bubble near the leading edge caused by the steep adverse pressure gradient after the peak on the nose. On the upper surface a laminar separation bubble is present which slowly moves forward with increasing angle of attack. At $\alpha < 10^0$ the laminar boundary layer separates in the destabilizing region before transition occurs and reattachment is in the steep part of the pressure recovery region. At $\alpha = 10^0$ transition is at the onset of the pressure recovery region and the drag is a minimum. Beyond $\alpha = 10^0$ the bubble moves forward in the destabilizing region, and at $\alpha = 11.7^0$ the maximum lift coefficient is reached; beyond that angle complete separation of the pressure recovery region occurs.

By increasing the Reynolds number the boundary layer becomes thinner and transition moves forward. The decrease of boundary layer thickness causes the change in effective airfoil contour indicated by the pressure distributions in Fig. 11 and corresponding slight lift increase in Fig. 9. Due to earlier transition the length of the laminar separation bubble decreases, Fig. 11, but so does the width of the low drag bucket and the maximum lift coefficient, Fig. 9.
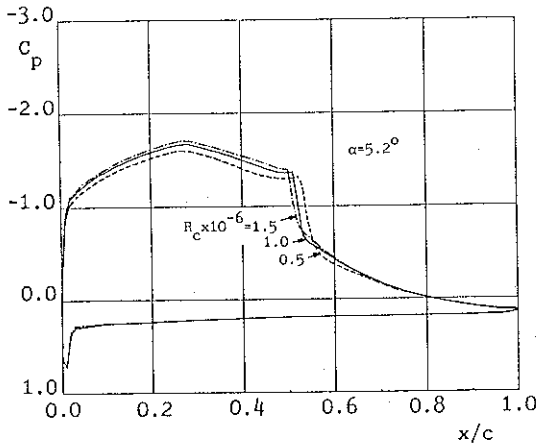
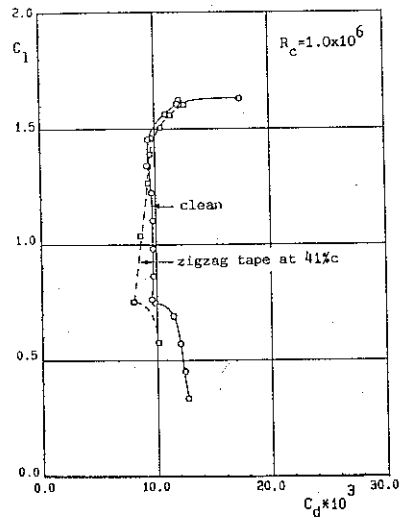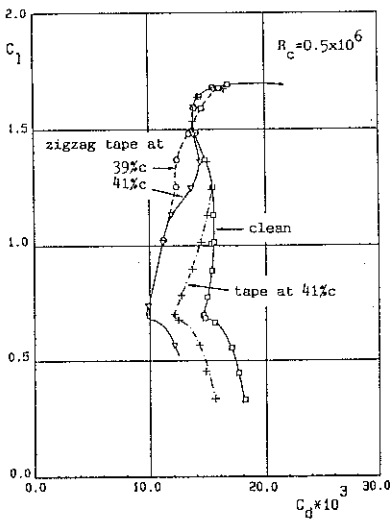Fig. 11 Measured pressure distributions of LA 5055

Fig. 12 Measured characteristics of LA 5055 with and without turbulators

Fig. 12 shows results of tests with <u>turbulators</u> on LA 5055. A strip of tape positioned at 41%c shows at $Re=0.5*10^6$ a drag reduction at lift coefficients below 1.25; at higher lift coefficients the tape is submerged in the laminar separation bubble. A zig-zag form, cut from the same tape and applied at the same chord position, is considerably more effective and produces a drag reduction up to 33%, but also submerges in the bubble at higher lift coefficients. Shifting the zig-zag tape 2%c forward makes it effective at all lift coefficients, with a drag penalty at lift coefficients near the upper end of the low drag bucket (probably transition occurs too early). Similar results are obtained at $Re=1*10^6$ and the zig-zag tape at 41%c.

The measured results illustrate both the difficulty..of designing and the negative effects of this type of destabilizing region where, ideally, the laminar boundary layer does not separate and transition occurs just at the end of the region. As explained in Ref. 4, this situation can only be obtained at one particular angle of attack and Reynolds number and deviations will cause transition to move forward on the destabilizing region or rearward, forming a bubble; either of which costs extra drag.

As illustrated in Ref. 9 and 10, it is favourable for the upper surface of an airfoil designed for sailplane application to design a pressure distribution which is rounded off in the transition region and, given the decrease of flight speed with increase of angle of attack, to exploit the destabilizing effect of the pressure gradient and at the same time the stabilizing effect of the Reynolds number to avoid the occurrence of a detrimental laminar separation bubble. On the lower surface the change in pressure gradient and Reynolds number have both stabilizing effects, and a rather long destabilizing region would be needed to avoid bubbles at the lower Reynolds number at the cost of a drag increase due to forward movement of transition at the higher Reynolds number. Here, and even more in case of airfoils designed for lower Reynolds numbers, artificial transition control provides a solution. The measurements on LA 5055 illustrate that for an effective application of artificial transition devices, the position of laminar separation should be fixed.
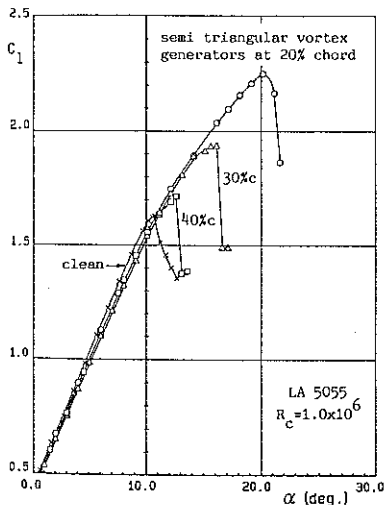

Fig. 13 Measured lift of LA 5055 with vortex generators
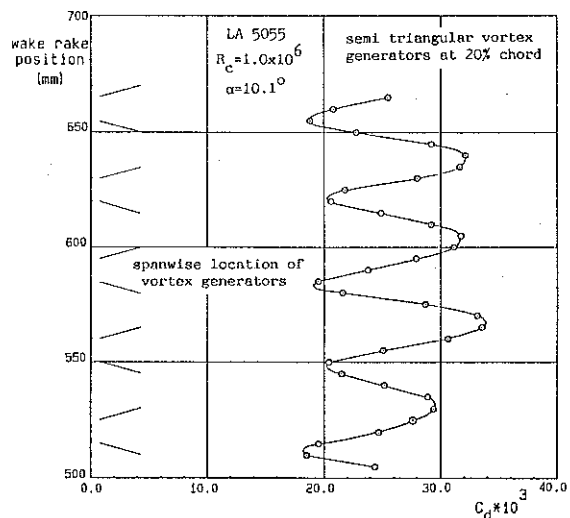
Fig. 14 Spanwise wake traverse measurements, LA 5055 with vortex generators

Tests with <u>vortex generators</u> on LA 5055 were performed in order to study the possibility of forced mixing in case of an imminent separation pressure recovery distribution, as suggested in Ref 11.

As shown by the results in Fig. 13 the maximum lift coefficient increases when the vortex generators are shifted forward. With the vortex generators at 20%c the maximum lift coefficient is raised by 38% with respect to the clean airfoil case. In all cases the turbulent boundary layer eventually separates at approximately 55%c due to the steep local pressure gradient. It is concluded that vortex generators postpone flow separation in case of Stratford type pressure recovery distributions provided that they are positioned some distance ahead of the separation point without generators. This conclusion is in accordance with the advice given by Taylor (Ref. 6) to locate the generators some 10 to 30 times the local boundary layer thickness upstream of the separation position without generators.

Fig. 14 shows results of spanwise wake traverse measurements. The periodicity of the results clearly shows the effects of the streamwise vortices emerging from the generators. The counter-rotating vortices of each pair of generators cause a decrease of boundary layer thickness at their centerline downstream, while the co-rotating vortices cause a thickening of the boundary layer between each pair of generators. The question arises how accurate the wake drag results are when vortices are present in the wake; comparison with balance measurements, as described in Ref. 12, would provide an answer. Anyhow, the results show again the necessity to do wake traverse measurements, which are very time consuming. Therefore, a computer controlled traversing wake rake system, using the 3-axis traversing system of the laboratory and applying ESP pressure scanners, is under development at LSL and will soon be available.
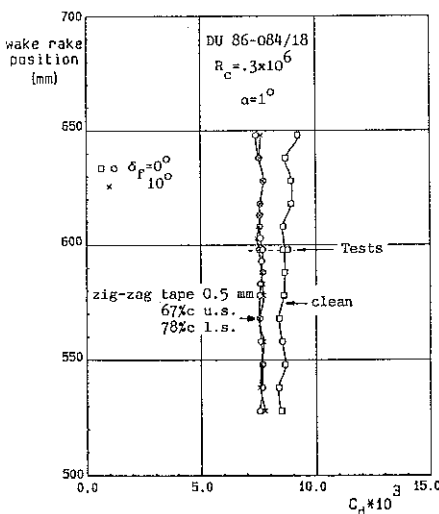

Fig. 15 Spanwise drag traverse measurements, DU 86-084/18

DU 86-084/18

In previous tests with different airfoils (Ref. 13) it was found that the lift measured with the balance system is independent of the width of the gap between the tip and lower reflection plate as long as this gap is smaller than 1 mm. This result was confirmed by tests with DU 86-084/18 where the gap was varied between 0.08 mm and 3 mm; the present results were obtained with the usual gap width of 0.5 mm. The model forces could be measured with negligible scatter by the balance system at Re = 100.000, however, the small pressure differences in the wake limited the drag measurements with the automatically reading multi-tube liquid manometer to Re = 200.000.

Spanwise drag surveys were made at several angles of attack and Reynolds numbers, both at zero and at ten degree flap deflection as well as without and with zig-zag tape. While the results without zig-zag tape show spanwise variations in drag coefficient up to 0.003 due to laminar separation bubbles on both sides of the airfoil, the results with zig-zag tape are nearly constant as illustrated in Fig. 15.

To find the best location and thickness of the zig-zag tape turbulators on the airfoil upper and lower surface, extensive systematic tests were performed at zero and ten degrees flap deflection and various Reynolds numbers. The final selection, being zig-zag tape of 0.5 mm thickness at 67%c upper surface and 78%c lower surface, produces the least drag at Reynolds numbers below 600.000. At higher Reynolds numbers there is a drag penalty (up to $\Delta c_d = 0.0005$ at Re=$1*10^6$) with respect to the lowest drag which could be obtained, being the price which has to be paid for these mechanical turbulators to be effective (not submerged) at low Reynolds numbers. Note that the Reynolds number for this airfoil varies with a factor 10.

Fig. 16 shows measured airfoil characteristics at two typical Reynolds numbers and flap deflections, without and with turbulators. The necessity and effectiveness of the turbulators is evident. At zero degree flap deflection the drag reduction is mainly due to the elimination of the bubble on the upper surface. At ten degrees flap deflection the turbulator on the lower surface is submerged in the bubble, as shown by oil flow studies, hence the large drag reduction is entirely due to the elimination of the bubble on the upper surface. No further drag reduction could be obtained at this flap deflection by changing the turbulator thickness and position on the lower surface; the drag already equals the drag at zero flap deflection as shown in Fig. 15. Hence, the presupposition in designing the airfoil that turbulator malfunction on the lower surface due to downward flap deflection would be harmless, has been substantiated.
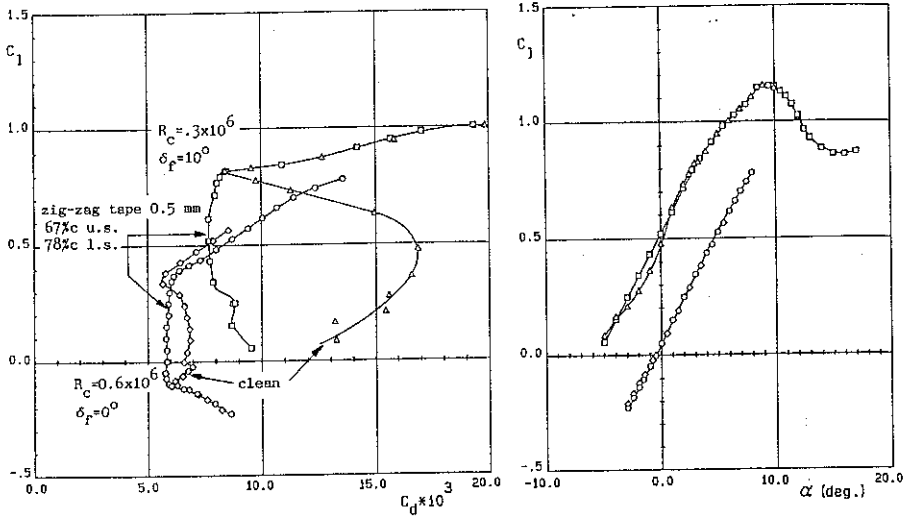
Fig. 16 Measured characteristics of DU 86-084/18 with and without zig-zag tape turbulators
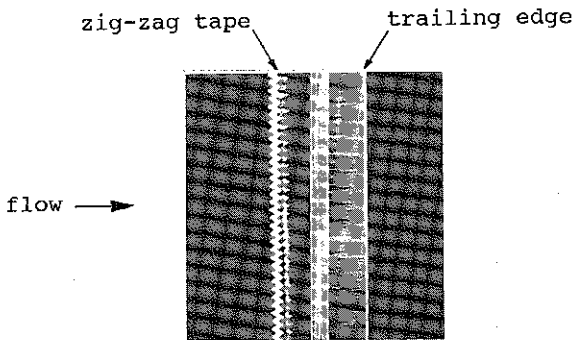

Fig. 17 Fluorescent oil flow pattern

The traces of the vortices produced by the zig-zag tape are clearly visible in the fluorescent oil flow pattern, an example of which is shown in Fig. 17.

Fig. 18 presents the characteristics for zero and ten degree flap deflection at relevant Reynolds numbers. The reproduction of the drag values at Re = 300.000 and higher is excellent, however the data at Re = 200.000 show scatter for reasons mentioned before. The gradient of the lift curves change when transition is moving forward and the drag increases. At ten degrees flap deflection the lift curve shows a small irregularity just before the maximum lift coefficient is reached; flow patterns revealed that this is due to a short bubble on the airfoil's nose which turns into a long bubble at increasing angle of attack. This also happens at the zero flap setting although it is

not noticeable in the lift curve. The stalling behaviour of the airfoil is gradual and no hysteresis loops were detected by increasing and decreasing the angle of attack.

Fig. 19 shows the effects of flap deflection at Re = 300.000. At $\delta = 15^0$ the upper limit of the low drag bucket is near $C_\ell = 1.0$ where the lift curve shows a small horizontal step and no dip as intended. At $\alpha = 7^0$ the short bubble on the airfoil's nose changes into a long

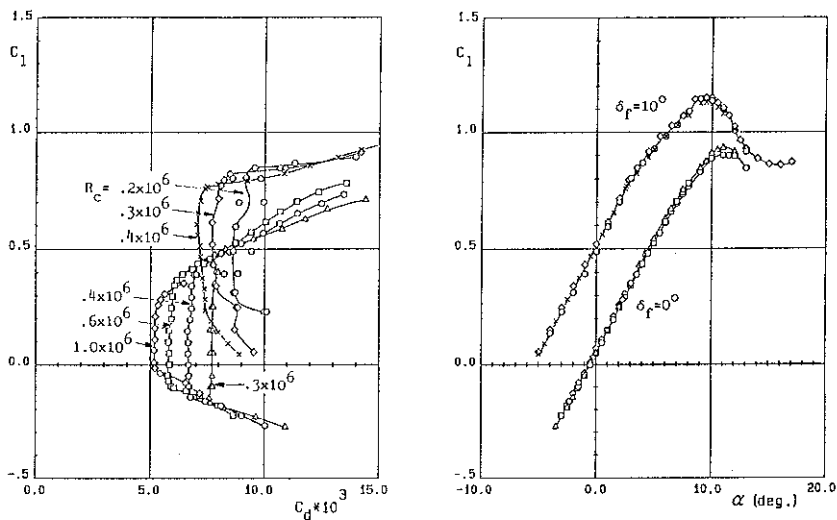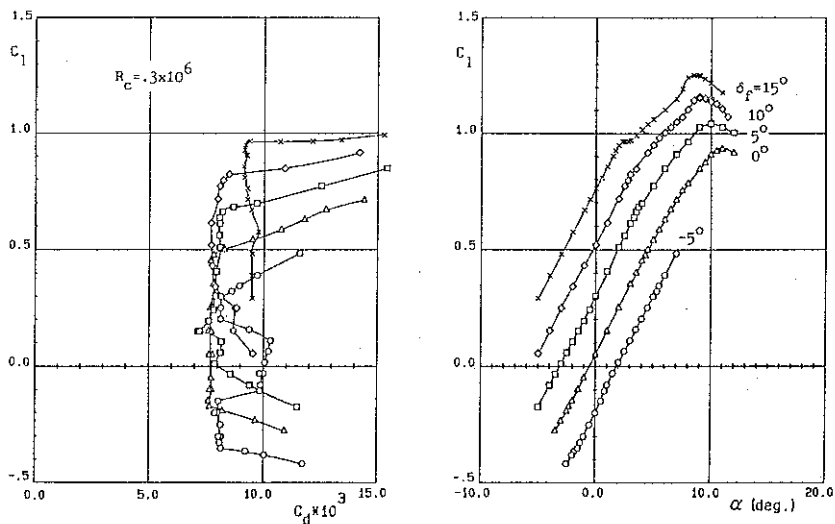Fig. 18   Measured characteristics of DU 86-084/18 with 0.5 mm zig-zag tape at 67%c u.s. and 78%c l.s.

Fig. 19   Measured characteristics of DU 86-084/18 with 0.5 mm zig-zag tape at 67%c u.s. and 78%c l.s.

bubble. At $\delta = -5^0$ there is turbulator malfunction on the upper surface; the pressures induced by this negative flap deflection cause laminar separation ahead of the turbulator which in turn submerges in the separated bubble flow. Contrary to the situation on the lower surface at positive flap deflections, there is a drag increase, which can be eliminated by shifting the turbulator forward or increase its thickness, but both measures have a drag penalty at higher Reynolds numbers. Pneumatic turbulators (blowing a small amount of air through orifices periodically spaced in spanwise direction) have the advantage that they are still active in the region behind laminar separation because the air jets pass through this region and disturb the laminar outer flow (Ref. 4). In view of this self-adjusting capability, it is intended to test the DU 86-084/18 airfoil with pneumatic turbulators, located further backward than the zig-zag tape turbulators, in order to see if a further drag reduction is possible.

4. References

1. Ingen, J.L. van, Boermans, L.M.M. and Blom, J.J.H.: Low speed airfoil section research at Delft University of Technology. ICAS-80-10.1, Munich, 1980.
2. Ingen, J.L. van: On the analysis and design of low speed airfoils using potential flow methods and boundary layer theory. Report LR-365, Department of Aerospace Engineering, Delft University of Technology, 1982.
3. Ingen, J.L. van, Boermans, L.M.M.: Aerodynamics at low Reynolds numbers: A review of theoretical and experimental research at Delft University of Technology. Paper no. 1 in Proceedings of the International Conference on Aerodynamics at low Reynolds numbers, October 1986, R.A.S. London.
4. Horstmann, K.H., Quast, A. and Boermans, L.M.M.: Pneumatic turbulators - a device for drag reduction at Reynolds numbers below 5×10^6. Paper no. 20 in AGARD CP-365, Brussels, 1984.
5. Wentz, W.H. and Seetharam, H.C.: Development of a fowler flap system for a high performance general aviation airfoil. NASA CR-2443, 1974.
6. Taylor, H.D.: Summary report on vortex generators. Report R-052809, United Aircraft Corporation, Research Dept., 1950.
7. Jones, B.M.: Measurement of profile drag by the pitot-traverse method. R&M no. 1688, Brit. A.R.C., 1936.
8. Allen, H.J., Vincenti, W.G.: Wall interference in a two-dimensional flow windtunnel with consideration of the effect of compressibility. NACA Report 782, 1944.
9. Boermans, L.M.M., Selen, H.J.W.: Design and tests of airfoils for sailplanes with an application to the ASW-19B. ICAS-paper 82-5.5.2, 1982.
10. Boermans, L.M.M., Waibel, G.: Aerodynamic and structural design of the Standard Class sailplane ASW-24. ICAS-paper 88-2.7.2, 1988.
11. Schubauer, G.B., Spangenberg, W.G.: Forced mixing in boundary layers. Journal of Fluid Mechanics, Vol. 8, 1960.
12. Boermans, L.M.M., Borne, P.C.M. van den: Design and tests of a flexible sailwing airfoil for lightweight aircraft. OSTIV Publication XVIII, 1985.
13. Volkers, D.F.: Preliminary results of wind tunnel measurements on some airfoil sections at Reynolds numbers between $0.6*10^5$ and $5.0*10^5$. Memorandum M-276, Faculty of Aerospace Engineering, Delft University of Technology, 1977.